Computation of fields in multi-layered structures

*

Multi-layered structures are the basis of modern semiconductor based integrated circuits, and they have been a subject of considerable interest in theoretical studies to gain an understanding of electromagnetic fields [?]. Most commonly, the fields are found in terms of the dyadic Green functions (DGFs) of the environment, which defines the vector field distribution due to a vector point source [1]. Due to a current $\mathbf{J}$ distributed in a region defined by a surface, r', the surface fields are expressed as in terms of an inner product,

$$\mathbf{E} = \int\limits_{r'} \underline{\underline{\mathbf{G}}}^{\mathrm{EJ}}(\mathbf{r}|\mathbf{r}')\mathbf{J}(\mathbf{r}')\,\mathrm{d}r', \tag{1a}$$

$$\mathbf{H} = \int\limits_{r'} \underline{\underline{\mathbf{G}}}^{\mathrm{HJ}}(\mathbf{r}|\mathbf{r}')\mathbf{J}(\mathbf{r}')\,\mathrm{d}r'. \tag{1b}$$

where, $\underline{\underline{\mathbf{G}}}^{\mathrm{EJ}}$ and $\underline{\underline{\mathbf{G}}}^{\mathrm{HJ}}$ are the spatial domain DGF's due to an electric current source located at r', that define the electric and magnetic fields at a point r respectively. In the presence of magnetic sources, (1a) and (1b) can be augmented using the superposition principle, by adding an inner product containing magnetic DGFs, $\underline{\underline{\mathbf{G}}}^{\mathrm{EM}}$ and $\underline{\underline{\mathbf{G}}}^{\mathrm{HM}}$.

*Last Modified: 17:13, Monday 29^{th} May, 2017.

1 Theory

We follow the well-established approach of field computation for planar multi-layered media [2, 3], in which, first an equivalent transmission line network is set up for the structure, and then transmission line Green function are computed.

1.1 Transmission line representation of Maxwell's equations

As shown in Fig. 3a, it is assumed that the structure is unbounded in the lateral direction, and excited only by an electric source. The electric and magnetic fields are given by the Maxwell's equations in frequency-domain,

$$\nabla \times \mathbf{E} = -j\omega\mu\mathbf{H}, \tag{2a}$$

$$\nabla \times \mathbf{H} = j\omega\varepsilon\mathbf{E} + \mathbf{J}. \tag{2b}$$

For boundary-value problems displaying symmetry along the z direction, it is desirable to decompose the ∇ operator into two components, one d/dz and the other a transverse (to z) operator, $\nabla_{\mathbf{t}}$ [4, p. 64]. By taking the Fourier transform,

$$\mathcal{F}[f(\rho, z)] \equiv \tilde{F}(\mathbf{k}_\rho, z) = \int_{-\infty}^{\infty}\int_{-\infty}^{\infty} f(\rho, z)\mathrm{e}^{-\mathrm{j}\mathbf{k}_\rho\cdot\rho}\,\mathrm{d}x\,\mathrm{d}y \tag{3}$$

the field computation is considerably simplified by switching to the spectral frequency domain $\mathbf{k}_\rho$, which reduces the complexity of the vector differential operator, ∇ to $-\mathrm{j}k_x\hat{\mathbf{x}} - \mathrm{j}k_y\hat{\mathbf{y}} + d/dz\,\hat{\mathbf{z}}$, which contains a derivative term only in z-direction. In (3), the cylindrical coordinates are expressed as,

$$\rho = x\hat{\mathbf{x}} + y\hat{\mathbf{y}}, \quad \text{and} \quad \mathbf{k}_\rho = k_x\hat{\mathbf{x}} + k_y\hat{\mathbf{y}}, \tag{4}$$

and the notation $\sim$ above the capital-letter terms indicates the Fourier transform with respect to the transverse coordinates and from here on, will be used to denote the spectral domain quantities.

As stated earlier, it is advantageous to separate the fields in transverse and longitudinal coordinates because, as we shall see shortly, the longitudinal part of the field can be completely expressed in terms of the transverse component. Applying the Fourier transform (3) on the Maxwell's equations (2), we obtain:

$$\left(-\mathrm{j}\mathbf{k}_\rho + \hat{\mathbf{z}}\frac{\mathrm{d}}{\mathrm{d}z}\right) \times (\tilde{\mathbf{E}}_t + \tilde{\mathbf{E}}_z) = -\mathrm{j}\omega\mu(\tilde{\mathbf{H}}_t + \tilde{\mathbf{H}}_z), \tag{5a}$$

$$\left(-\mathrm{j}\mathbf{k}_\rho + \hat{\mathbf{z}}\frac{\mathrm{d}}{\mathrm{d}z}\right) \times (\tilde{\mathbf{H}}_t + \tilde{\mathbf{H}}_z) = \mathrm{j}\omega\varepsilon(\tilde{\mathbf{E}}_t + \tilde{\mathbf{E}}_z) - (\tilde{\mathbf{J}}_t + \tilde{\mathbf{J}}_z). \tag{5b}$$

The transverse and longitudinal components of the magnetic field can be separately expressed in (5a) as,

$$-\mathrm{j}\mathbf{k}_\rho \times \tilde{\mathbf{E}}_z + \frac{\mathrm{d}}{\mathrm{d}z}\hat{\mathbf{z}} \times \tilde{\mathbf{E}}_t = -\mathrm{j}\omega\mu\tilde{\mathbf{H}}_t, \tag{6a}$$

$$-\mathrm{j}\mathbf{k}_\rho \times \tilde{\mathbf{E}}_t = -\mathrm{j}\omega\mu\tilde{\mathbf{H}}_z. \tag{6b}$$

Using the vector product property [5, p. 117],

$$\mathbf{A} \times \mathbf{B} = \mathbf{A} \cdot (\mathbf{B} \times \hat{\mathbf{n}})\, \hat{\mathbf{n}}, \tag{7}$$

where the unit vector $\hat{\mathbf{n}}$ is normal to the plane containing vectors $\mathbf{A}$ and $\mathbf{B}$. A scalar form of the longitudinal component of the electric field is obtained by applying (7) on (6b),

$$-\mathrm{j}\mathbf{k}_\rho \cdot (\tilde{\mathbf{E}}_t \times \hat{\mathbf{z}})\, \hat{\mathbf{z}} = -\mathrm{j}\omega\mu\tilde{\mathbf{H}}_z \tag{8}$$

which can be written in the scalar form,

$$-\mathrm{j}\tilde{H}_z = \frac{-\mathrm{j}}{\omega\mu}\mathbf{k}_\rho \cdot (\tilde{\mathbf{E}}_t \times \hat{\mathbf{z}}). \tag{9}$$

Now taking the vector product with unit vector $\hat{\mathbf{z}}$ on both sides of (6a), the transverse electric field component is expressed as:

$$\begin{aligned} \frac{\mathrm{d}\tilde{\mathbf{E}}_t}{\mathrm{d}z} &= -\mathrm{j}(\mathbf{k}_\rho \times \tilde{\mathbf{E}}_z) \times \hat{\mathbf{z}} - \mathrm{j}\omega\mu\tilde{\mathbf{H}}_t \times \hat{\mathbf{z}} \\ &= -\mathrm{j}\mathbf{k}_\rho\tilde{E}_z - \mathrm{j}\omega\mu\tilde{\mathbf{H}}_t \times \hat{\mathbf{z}} \end{aligned} \tag{10}$$

where the BAC-CAB vector triple product identity, $(\mathbf{A}\times\mathbf{B})\times\mathbf{C} \equiv \mathbf{B}(\mathbf{A}\cdot\mathbf{C}) - \mathbf{C}(\mathbf{A}\cdot\mathbf{B})$ has been applied.

Following a similar procedure starting from (5b), we obtain the transverse component of magnetic field, along with the scalar longitudinal component of electric field:

$$
\begin{aligned}
\frac{\mathrm{d}\tilde{\mathbf{H}}_t}{\mathrm{d}z} &= -\mathrm{j}(\mathbf{k}_\rho \times \tilde{\mathbf{H}}_z) \times \hat{\mathbf{z}} + \mathrm{j}\omega\varepsilon \tilde{\mathbf{E}}_t \times \hat{\mathbf{z}} + \tilde{\mathbf{J}}_t \times \hat{\mathbf{z}} \\
&= -\mathrm{j}\mathbf{k}_\rho \tilde{H}_z + \mathrm{j}\omega\varepsilon \tilde{\mathbf{E}}_t \times \hat{\mathbf{z}} + \tilde{\mathbf{J}}_t \times \hat{\mathbf{z}},
\end{aligned}
\tag{11}
$$

and,

$$
-\mathrm{j}\omega\varepsilon \tilde{E}_z = \mathrm{j}\mathbf{k}_\rho \cdot (\tilde{\mathbf{H}}_t \times \hat{\mathbf{z}}) + \tilde{J}_z. \tag{12}
$$

By substituting (12) in (10), we get the transverse component of electric field,

$$
\frac{\mathrm{d}\tilde{\mathbf{E}}_t}{\mathrm{d}z} = \frac{1}{\mathrm{j}\omega\varepsilon}\left(k^2 - \mathbf{k}_\rho \mathbf{k}_\rho \cdot\right)(\tilde{\mathbf{H}}_t \times \hat{\mathbf{z}}) + \mathbf{k}_\rho \frac{\tilde{J}_z}{\omega\varepsilon}. \tag{13}
$$

Similarly, from (9) and (11), the transverse component of magnetic field,

$$
\frac{\mathrm{d}\tilde{\mathbf{H}}_t}{\mathrm{d}z} = \frac{1}{\mathrm{j}\omega\mu}\left(k^2 - \mathbf{k}_\rho \mathbf{k}_\rho \cdot\right)(\hat{\mathbf{z}} \times \tilde{\mathbf{E}}_t) + \tilde{\mathbf{J}}_t \times \hat{\mathbf{z}} \tag{14}
$$

where $k = \omega\sqrt{\mu\varepsilon}$ in (13) and (14) is the medium wavenumber.

The fields in (13) and (14) for arbitrarily aligned sources lie in the plane of a spectral coordinate system as illustrated in Fig. 1, where the arrowheads in color correspond to spectral-domain quantities. A rotational transformation of the coordinate system such that the axes align with the vectors $\mathbf{k}_\rho, \hat{\mathbf{z}} \times \mathbf{k}_\rho$ [6], simplifies the procedure of finding the transmission line equivalent, which allows the TE and TM mode analysis to be made separately. The coordinate transformation can be expressed as:

$$
\begin{bmatrix} \hat{\mathbf{u}} \\ \hat{\mathbf{v}} \end{bmatrix} = \begin{bmatrix} \cos\psi & \sin\psi \\ -\sin\psi & \cos\psi \end{bmatrix} \begin{bmatrix} \hat{\mathbf{x}} \\ \hat{\mathbf{y}} \end{bmatrix} \tag{15}
$$

where ψ is the angle between $\mathbf{k}_\rho$ and the positive x-axis. A transmission line analogue for the spectral fields, expressed in terms of modal voltages and currents can therefore, be written as [7, 3],

$$
\begin{bmatrix} \tilde{\mathbf{E}}_t \\ \tilde{\mathbf{H}}_t \end{bmatrix} = \begin{bmatrix} V^{\mathrm{TM}} & V^{\mathrm{TE}} \\ -I^{\mathrm{TE}} & I^{\mathrm{TM}} \end{bmatrix} \begin{bmatrix} \hat{\mathbf{u}} \\ \hat{\mathbf{v}} \end{bmatrix}. \tag{16}
$$

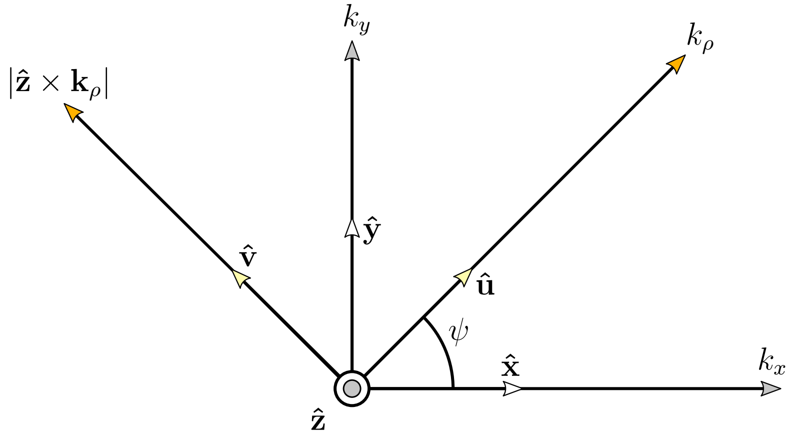

Figure 1: Coordinate System transformation in the spectral domain

Using the results of (16) in (13) and noting that $\hat{\mathbf{u}} = \mathbf{k}_\rho / k_\rho$, we get,

$$\frac{\mathrm{d}\left(\hat{\mathbf{u}}\, V^{\mathrm{TM}} + \hat{\mathbf{v}}\, V^{\mathrm{TE}}\right)}{\mathrm{d}z} = \frac{1}{\mathrm{j}\omega\varepsilon}\left(k^2 - \mathbf{k}_\rho\, \mathbf{k}_\rho\, \cdot\right)\left(\hat{\mathbf{u}}\, I^{\mathrm{TM}} + \hat{\mathbf{v}}\, I^{\mathrm{TE}}\right) + \hat{\mathbf{u}}\, \frac{k_\rho}{\omega\varepsilon} \tilde{J}_z \tag{17}$$

By separating the $\hat{\mathbf{u}}$ and $\hat{\mathbf{v}}$ components, we obtain the TM and TE equivalent voltage equations respectively,

$$\frac{\mathrm{d}V^{\mathrm{TM}}}{\mathrm{d}z} = \frac{1}{\mathrm{j}\omega\varepsilon}\left(k^2 - k_\rho^2\right) I^{\mathrm{TM}} + \frac{k_\rho}{\omega\varepsilon}\tilde{J}_z, \tag{18a}$$

$$\frac{\mathrm{d}V^{\mathrm{TE}}}{\mathrm{d}z} = \frac{k^2}{\mathrm{j}\omega\varepsilon} I^{\mathrm{TE}}. \tag{18b}$$

Similarly, from (16) and (14), the equivalent current equations can be written as:

$$\frac{\mathrm{d}I^{\mathrm{TM}}}{\mathrm{d}z} = \frac{k^2}{\mathrm{j}\omega\mu} V^{\mathrm{TM}} - \tilde{J}_u, \tag{19a}$$

$$\frac{\mathrm{d}I^{\mathrm{TE}}}{\mathrm{d}z} = \frac{-1}{\mathrm{j}\omega\mu}\left(k^2 - k_\rho^2\right) V^{\mathrm{TE}} + \tilde{J}_v. \tag{19b}$$

Equations (18)-(19) can be conveniently written in a compact form as a set of telegrapher's equations [4, p. 190]:

$$\frac{\mathrm{d}V^\alpha}{\mathrm{d}z} = -\mathrm{j}k_z Z^\alpha I^\alpha + v^\alpha \tag{20a}$$

$$\frac{\mathrm{d}I^\alpha}{\mathrm{d}z} = -\mathrm{j}k_z Y^\alpha V^\alpha + i^\alpha \tag{20b}$$

where α is either TE or TM, the propagation constant in the transverse direction is $k_z = \pm\sqrt{k^2 - k_\rho^2}$, for which the sign must be chosen in such a way the fields decay away from the source. The modal impedances in (20) are,

$$Z^{\mathrm{TM}} = \frac{1}{Y^{\mathrm{TM}}} = \frac{k_z}{\omega\varepsilon}, \tag{21a}$$

$$Z^{\mathrm{TE}} = \frac{1}{Y^{\mathrm{TE}}} = \frac{\omega\mu}{k_z}. \tag{21b}$$

Using the expressions that relate the transverse electric and mangnetic to the equivalent transmission line currents and voltages (16), and combining with the longitudinal field expressions (6b) and (12), we obtain the total fields in the spectral domain,

$$\begin{bmatrix} \tilde{\mathbf{E}}(\mathbf{k}_\rho, z) \\ \tilde{\mathbf{H}}(\mathbf{k}_\rho, z) \end{bmatrix} = \begin{bmatrix} V^{\mathrm{TM}} & V^{\mathrm{TE}} & -\frac{k_\rho}{\omega\varepsilon(z)} I^{\mathrm{TM}}(z) \\ -I^{\mathrm{TE}} & I^{\mathrm{TM}} & \frac{k_\rho}{\omega\mu} V^{\mathrm{TE}}(z) \end{bmatrix} \begin{bmatrix} \hat{\mathbf{u}} \\ \hat{\mathbf{v}} \\ \hat{\mathbf{z}} \end{bmatrix} + \hat{\mathbf{z}} \begin{bmatrix} \frac{\mathrm{j}}{\omega\varepsilon(z)} \tilde{\mathbf{J}}_z(\mathbf{k}_\rho, z) \\ 0 \end{bmatrix}, \tag{22}$$

where $\varepsilon(z)$ may vary from one layer to another.

Assuming only electric sources existing in space, the corresponding TL sources, v^α and i^α, defined in (20), are illustrated in 2. A horizontally oriented (x-directed) electric dipole is represented by a current source in an equivalent TM transmission line network. Likewise, the equivalent configuration of a vertical (y-directed) electric dipole is a TE network with a current source. A z-directed dipole corresponds to voltage source in a TM transmission line. For an arbitrarily directed source, the equivalent TL model consists of a superposition of the three representations.

1.2 Green functions for the TL equations

To obtain the transmission-line voltages and currents that define the spectral fields in (22), we introduce the one-dimensional transmission-line Green functions (TLGFs) that are analogous to the spatial domain DGFs in (1). Following [4, 2], we define $V_i(z, z')$ and $I_i(z, z')$ as the voltage and current respectively, at a point z along the transmission line due to a unit-strength current source located at z'. Similarly, $V_v(z, z')$ and $I_v(z, z')$ are the respective voltage and current due to a unit-strength

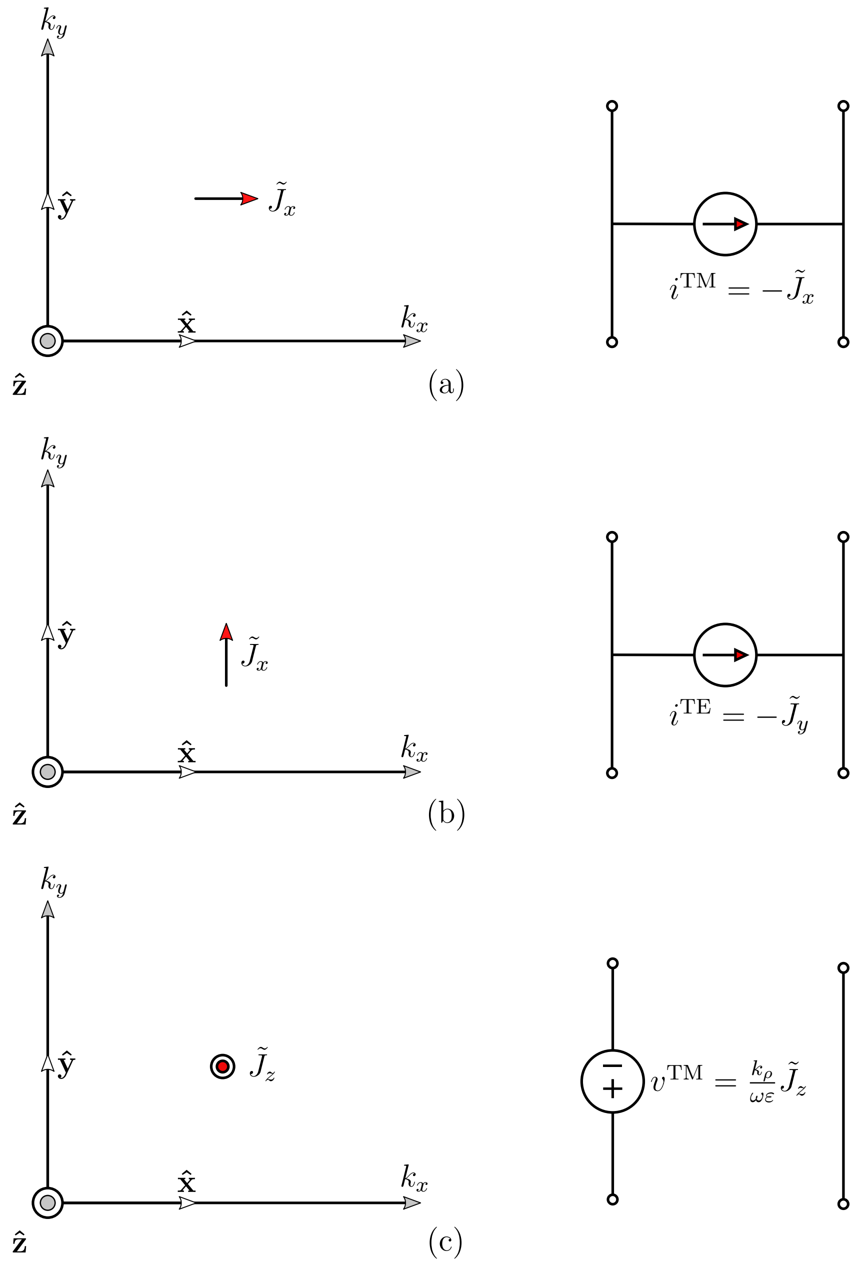

Figure 2: Electric Source representation in a transmission line network

voltage source. Analogous to (1) which is augmented by magnetic sources, we write:

$$V(z) = \int\limits_{z'} \left[V_i(z,z')i(z') + V_v(z,z')v(z')\right] \mathrm{d}z', \tag{23a}$$

$$I(z) = \int\limits_{z'} \left[I_i(z,z')i(z') + I_v(z,z')v(z')\right] \mathrm{d}z'. \tag{23b}$$

The telegrapher's equations (20), are rewritten for a voltage excited line as:

$$\frac{\mathrm{d}V_v}{\mathrm{d}z} = -\mathrm{j}k_z Z_v I_v + \delta(z - z') \tag{24a}$$

$$\frac{\mathrm{d}I_v}{\mathrm{d}z} = -\mathrm{j}k_z Y_v V_v, \tag{24b}$$

and for a current excited line, we obtain:

$$\frac{\mathrm{d}V_i}{\mathrm{d}z} = -\mathrm{j}k_z Z_i I_i \tag{25a}$$

$$\frac{\mathrm{d}I_i}{\mathrm{d}z} = -\mathrm{j}k_z Y_i V_i + \delta(z - z') \tag{25b}$$

1.3 Spectral Domain Dyadic Green Functions

By substituting (24) and (25) into (22) and referring to Fig. 2, we obtain the spectral-domain versions of DGFs [3]:

$$\begin{aligned}\underline{\underline{\tilde{\mathbf{G}}}}^{\mathrm{EJ}}(\mathbf{k}_\rho, z|z') = & -\hat{\mathbf{u}}\hat{\mathbf{u}}V_i^{\mathrm{TM}} - \hat{\mathbf{v}}\hat{\mathbf{v}}V_i^{\mathrm{TE}} + \hat{\mathbf{z}}\hat{\mathbf{u}}\frac{k_\rho}{\omega\varepsilon(z)}I_i^{\mathrm{TM}} \\ & + \hat{\mathbf{u}}\hat{\mathbf{z}}\frac{k_\rho}{\omega\varepsilon(z')}V_v^{\mathrm{TM}} + \hat{\mathbf{z}}\hat{\mathbf{z}}\frac{1}{\mathrm{j}\omega\varepsilon(z')}\left[\frac{k_\rho^2}{\mathrm{j}\omega\varepsilon(z)}I_v^{\mathrm{TM}} - \delta(z - z')\right],\end{aligned} \tag{26a}$$

$$\underline{\underline{\tilde{\mathbf{G}}}}^{\mathrm{HJ}}(\mathbf{k}_\rho, z|z') = \hat{\mathbf{u}}\hat{\mathbf{v}}I_i^{\mathrm{TE}} - \hat{\mathbf{v}}\hat{\mathbf{u}}I_i^{\mathrm{TE}} - \hat{\mathbf{z}}\hat{\mathbf{v}}\frac{k_\rho}{\omega\mu}V_i^{\mathrm{TE}} + \hat{\mathbf{v}}\hat{\mathbf{z}}\frac{k_\rho}{\omega\varepsilon(z')}I_v^{\mathrm{TM}}. \tag{26b}$$

1.4 Spatial Domain Dyadic Green Functions

By taking an inverse Fourier transform (27),

$$\mathcal{F}^{-1}[\tilde{F}(\mathbf{k}_\rho, z)] \equiv f(\rho, z) = \frac{1}{(2\pi)^2}\int\limits_{-\infty}^{\infty}\int\limits_{-\infty}^{\infty} \tilde{F}(\mathbf{k}_\rho, z)\mathrm{e}^{\mathrm{j}\mathbf{k}_\rho\cdot\rho}\,\mathrm{d}k_x\,\mathrm{d}k_y. \tag{27}$$

we find the spatial domain analogues of the spectral domain DGFs, which are defined in (26). In case of rotational symmetry which implies that $\tilde{F}$ only depends on one spectral co-ordinate k_ρ, the double integral in (27) can be simplified to an integral of only one variable. Using (4) and the coordinate transformation shown in Fig. 1 where,

$$k_x = k_\rho \cos\psi \qquad \text{and} \qquad k_y = k_\rho \sin\psi, \tag{28}$$

we rewrite (27) in cylindrical coordinates,

$$\mathcal{F}^{-1}[\tilde{F}(\mathbf{k}_\rho, z)] \equiv f(\rho, z) = \frac{1}{(2\pi)^2} \int_0^\infty \int_0^{2\pi} \tilde{F}(\mathbf{k}_\rho, z) \mathrm{e}^{\mathrm{j}\mathbf{k}_\rho \cdot \boldsymbol{\rho}} k_\rho \, \mathrm{d}k_\rho \, \mathrm{d}\psi. \tag{29}$$

Applying the Fourier-Bessel transform (FBT) to (29) which states that,

$$\frac{1}{2\pi} \int_0^{2\pi} \mathrm{e}^{\mathrm{j}\mathbf{k}_\rho \cdot \boldsymbol{\rho}} \, \mathrm{d}\psi = J_0(k_\rho \rho), \tag{30}$$

where $J_0(\cdot)$ is the Bessel function of zero order we obtain the Sommerfeld integral (SI), $\mathcal{S}_0\{\cdot\}$:

$$f(\rho) = \mathcal{S}_0\left\{\tilde{F}\right\} \equiv \frac{1}{2\pi} \int_0^\infty J_0(k_\rho \rho) \tilde{F}(k_\rho) k_\rho \, \mathrm{d}k_\rho. \tag{31}$$

In some cases, the Bessel function may be up to an order of 2, therefore, generalized expression for SI is,

$$\mathcal{S}_n\left\{\tilde{F}\right\} \equiv \frac{1}{2\pi} \int_0^\infty J_n(k_\rho \rho) \tilde{F}(k_\rho) k_\rho \, \mathrm{d}k_\rho. \tag{32}$$

Following the above procedure, we write the spatial domain DGFs as:

$$\underline{\underline{\mathbf{G}}}^\kappa(\rho, z|z') = \mathcal{F}^{-1}\left[\underline{\underline{\tilde{\mathbf{G}}}}^\kappa(\mathbf{k}_\rho, z|z')\right] \equiv \mathcal{S}_n\left\{\underline{\underline{\tilde{\mathbf{G}}}}^\kappa(\mathbf{k}_\rho, z|z')\right\} \tag{33}$$

where the superscript κ denotes either EJ or HJ.

Starting with (26), we now discuss each step in detail to obtain the spatial domain versions of the DGFs. First, the spectral domain dyads are converted to their spatial domain counterparts using the relations listed in Table 1 which are obtained from Fig. 1 and (15). In general, a spatial domain DGF can be expressed in a matrix

Spectral domain dyad	Spatial domain dyad
$\hat{\mathbf{u}}\hat{\mathbf{u}}$	$\hat{\mathbf{x}}\hat{\mathbf{x}}\cos^2\psi + \hat{\mathbf{x}}\hat{\mathbf{y}}\cos\psi\,\sin\psi + \hat{\mathbf{y}}\hat{\mathbf{x}}\cos\psi\,\sin\psi + \hat{\mathbf{y}}\hat{\mathbf{y}}\sin^2\psi$
$\hat{\mathbf{v}}\hat{\mathbf{v}}$	$\hat{\mathbf{x}}\hat{\mathbf{x}}\sin^2\psi - \hat{\mathbf{x}}\hat{\mathbf{y}}\cos\psi\,\sin\psi - \hat{\mathbf{y}}\hat{\mathbf{x}}\cos\psi\,\sin\psi + \hat{\mathbf{y}}\hat{\mathbf{y}}\sin^2\psi$
$\hat{\mathbf{u}}\hat{\mathbf{v}}$	$-\hat{\mathbf{x}}\hat{\mathbf{x}}\cos\psi\,\sin\psi + \hat{\mathbf{x}}\hat{\mathbf{y}}\cos^2\psi - \hat{\mathbf{y}}\hat{\mathbf{x}}\sin^2\psi + \hat{\mathbf{y}}\hat{\mathbf{y}}\cos\psi\,\sin\psi$
$\hat{\mathbf{v}}\hat{\mathbf{u}}$	$-\hat{\mathbf{x}}\hat{\mathbf{x}}\cos\psi\,\sin\psi - \hat{\mathbf{x}}\hat{\mathbf{y}}\sin^2\psi + \hat{\mathbf{y}}\hat{\mathbf{x}}\cos^2\psi + \hat{\mathbf{y}}\hat{\mathbf{y}}\cos\psi\,\sin\psi$
$\hat{\mathbf{z}}\hat{\mathbf{u}}$	$\hat{\mathbf{z}}\hat{\mathbf{x}}\cos\psi + \hat{\mathbf{z}}\hat{\mathbf{y}}\sin\psi$
$\hat{\mathbf{u}}\hat{\mathbf{z}}$	$\hat{\mathbf{x}}\hat{\mathbf{z}}\cos\psi + \hat{\mathbf{y}}\hat{\mathbf{z}}\sin\psi$
$\hat{\mathbf{z}}\hat{\mathbf{v}}$	$-\hat{\mathbf{z}}\hat{\mathbf{x}}\sin\psi + \hat{\mathbf{z}}\hat{\mathbf{y}}\cos\psi$
$\hat{\mathbf{v}}\hat{\mathbf{z}}$	$-\hat{\mathbf{x}}\hat{\mathbf{z}}\sin\psi + \hat{\mathbf{y}}\hat{\mathbf{z}}\cos\psi$

Table 1: Conversion of spectral domain dyad to spatial domain

form:

$$\underline{\underline{\mathbf{G}}}^{\kappa} = \begin{bmatrix} G^{\kappa}_{xx} & G^{\kappa}_{xy} & G^{\kappa}_{xz} \\ G^{\kappa}_{yx} & G^{\kappa}_{yy} & G^{\kappa}_{yz} \\ G^{\kappa}_{zx} & G^{\kappa}_{zy} & G^{\kappa}_{zz} \end{bmatrix}, \tag{34}$$

As an example, we consider the spatial domain component, G^{EJ}_{xx} of the DGF, which can be expressed as:

$$\begin{aligned} G^{\mathrm{EJ}}_{xx} &= \mathcal{F}^{-1}\left\{-\cos^2\psi V_i^{\mathrm{TM}} - \sin^2\psi V_i^{\mathrm{TE}}\right\} \\ &= -\mathcal{F}^{-1}\left\{\frac{1+\cos 2\psi}{2}V_i^{\mathrm{TM}} + \frac{1-\cos 2\psi}{2}V_i^{\mathrm{TE}}\right\} \\ &= -\frac{1}{2}\mathcal{S}_0\left\{V_i^{\mathrm{TM}} + V_i^{\mathrm{TE}}\right\} - \mathcal{F}^{-1}\left\{\frac{\cos 2\psi}{2}V_i^{\mathrm{TM}} - V_i^{\mathrm{TE}}\right\} \end{aligned} \tag{35}$$

Using the formula [2],

$$\mathcal{F}^{-1}\left\{\cos 2\psi\,\tilde{F}\right\} = -\cos 2\phi\,\mathcal{S}_2\left\{\tilde{F}\right\} \tag{36}$$

and the recurrence relation for Bessel-type functions [8],

$$J_{n+1}(z) = \frac{2n}{z} J_n(z) - J_{n-1}(z) \tag{37}$$

(35) is simplified to:

$$\begin{aligned} G_{xx}^{\text{EJ}} &= -\frac{1}{2}\mathcal{S}_0\left\{V_i^{\text{TM}}\right\} - \frac{1}{2}\mathcal{S}_0\left\{V_i^{\text{TE}}\right\} + \frac{\cos 2\phi}{2}\mathcal{S}_2\left\{V_i^{\text{TM}} - V_i^{\text{TE}}\right\} \\ &= -\frac{1}{2}\mathcal{S}_0\left\{V_i^{\text{TM}}\right\} - \frac{1}{2}\mathcal{S}_0\left\{V_i^{\text{TE}}\right\} + \frac{\cos 2\phi}{2}\left[\frac{2}{\rho}\mathcal{S}_1\left\{V_i^{\text{TM}} - V_i^{\text{TE}}\right\} - \mathcal{S}_0\left\{V_i^{\text{TM}} - V_i^{\text{TE}}\right\}\right]. \end{aligned} \tag{38}$$

After some algebraic manipulation and knowing the fact that Sommerfeld integrals obey the linearity principle, we obtain the final expression:

$$G_{xx}^{\text{EJ}} = -\cos^2\phi\,\mathcal{S}_0\left\{V_i^{\text{TM}}\right\} - \sin^2\phi\,\mathcal{S}_0\left\{V_i^{\text{TE}}\right\} + \frac{\cos 2\phi}{2}\mathcal{S}_2\left\{V_i^{\text{TM}} - V_i^{\text{TE}}\right\}. \tag{39}$$

Following similar procedure, the remaining components of both electric and magnetic fields DGFs in the spatial domain can be obtained, which are listed in Table. 2 [2].

1.5 Introducing Potential functions

As evident in Tables 2 and 3, the spatial domain DGFs that directly describe fields are tedious. An alternative formulation using vector potential functions considerably reduces the computation complexity. The approach is commonly known as mixed potentials integral equation (MPIE) formulation. From the Maxwell's equations, we know that,

$$\nabla \cdot \mu\mathbf{H} = 0, \tag{40}$$

and using the vector identity, $\nabla\cdot(\nabla\times\mathbf{A}) \equiv 0$, we define the magnetic vector potential, A such that:

$$\mathbf{H} = \frac{1}{\mu}\nabla \times \mathbf{A}. \tag{41}$$

Through (2a) and (41), we write:

$$\nabla \times (\mathbf{E} + \mathrm{j}\omega\mathbf{A}) = 0, \tag{42}$$

GF	$\kappa = \mathrm{EJ}$
G_{xx}	$-\cos^2\psi\,\mathcal{S}_0\left\{V_i^{\mathrm{TM}}\right\} - \sin^2\psi\,\mathcal{S}_0\left\{V_i^{\mathrm{TE}}\right\} + \dfrac{\cos(2\psi)}{\rho}\mathcal{S}_1\left\{\dfrac{V_i^{\mathrm{TM}} - V_i^{\mathrm{TE}}}{k_\rho}\right\}$
G_{xy}	$-\dfrac{\sin(2\psi)}{2}\mathcal{S}_0\left\{V_i^{\mathrm{TM}} - V_i^{\mathrm{TE}}\right\} + \dfrac{\sin(2\psi)}{\rho}\mathcal{S}_1\left\{\dfrac{V_i^{\mathrm{TM}} - V_i^{\mathrm{TE}}}{k_\rho}\right\}$
G_{xz}	$\dfrac{\eta_0}{\mathrm{j}k_0\varepsilon(z')}\cos\psi\,\mathcal{S}_1\left\{k_\rho V_v^{\mathrm{TM}}\right\}$
G_{yx}	$-\dfrac{\sin(2\psi)}{2}\mathcal{S}_0\left\{V_i^{\mathrm{TM}} - V_i^{\mathrm{TE}}\right\} + \dfrac{\sin(2\psi)}{\rho}\mathcal{S}_1\left\{\dfrac{V_i^{\mathrm{TM}} - V_i^{\mathrm{TE}}}{k_\rho}\right\}$
G_{yy}	$-\sin^2\psi\,\mathcal{S}_0\left\{V_i^{\mathrm{TM}}\right\} - \cos^2\psi\,\mathcal{S}_0\left\{V_i^{\mathrm{TE}}\right\} - \dfrac{\cos(2\psi)}{\rho}\mathcal{S}_1\left\{\dfrac{V_i^{\mathrm{TM}} - V_i^{\mathrm{TE}}}{k_\rho}\right\}$
G_{yz}	$\dfrac{\eta_0}{\mathrm{j}k_0\varepsilon(z')}\sin\psi\,\mathcal{S}_1\left\{k_\rho V_v^{\mathrm{TM}}\right\}$
G_{zx}	$\dfrac{\eta_0}{\mathrm{j}k_0\varepsilon(z)}\cos\psi\,\mathcal{S}_1\left\{k_\rho I_i^{\mathrm{TM}}\right\}$
G_{zy}	$\dfrac{\eta_0}{\mathrm{j}k_0\varepsilon(z)}\sin\psi\,\mathcal{S}_1\left\{k_\rho I_i^{\mathrm{TM}}\right\}$
G_{zz}	$-\dfrac{\eta_0^2}{\mathrm{j}k_0^2\varepsilon(z)\varepsilon(z')}\mathcal{S}_0\left\{k_\rho^2 I_v^{\mathrm{TM}}\right\} - \dfrac{\eta_0}{\mathrm{j}k_0\varepsilon(z)}\delta(\rho)\delta(z-z')$

Table 2: Scalar Green functions for computation of electric field due to an electric current source [2]

and knowing the vector identity, $\nabla \times (-\nabla\phi) \equiv 0$, the electric field is expressed as:

$$\mathbf{E} = \mathrm{j}\omega\mathbf{A} - \nabla\phi. \tag{43}$$

The scalar potential function ϕ can be related to A by the Lorenz gauge, which states that:

$$\nabla \cdot \mathbf{A} = -\mathrm{j}\omega\mu\varepsilon\phi. \tag{44}$$

The electric field in (43) is then expressed only as a function of $\mathbf{A}$,

$$\mathbf{E} = \frac{\mathrm{j}\omega}{k^2}\left(k^2 + \nabla\nabla\cdot\right)\mathbf{A}. \tag{45}$$

For a current distribution $\mathbf{J}$, the vector potential $\mathbf{A}$ can also be described by a

GF	$\kappa = \mathrm{HJ}$
G_{xx}	$-\frac{\sin(2\psi)}{2}\mathcal{S}_0\left\{I_i^{\mathrm{TE}} - I_i^{\mathrm{TM}}\right\} + \frac{\sin(2\psi)}{\rho}\mathcal{S}_1\left\{\frac{I_i^{\mathrm{TE}} - I_i^{\mathrm{TM}}}{k_\rho}\right\}$
G_{xy}	$\cos^2\psi\,\mathcal{S}_0\left\{I_i^{\mathrm{TE}}\right\} + \sin^2\psi\,\mathcal{S}_0\left\{I_i^{\mathrm{TM}}\right\} - \frac{\cos(2\psi)}{\rho}\mathcal{S}_1\left\{\frac{I_i^{\mathrm{TE}} - I_i^{\mathrm{TM}}}{k_\rho}\right\}$
G_{xz}	$-\frac{\eta_0}{\mathrm{j}k_0\varepsilon(z)}\sin\psi\,\mathcal{S}_1\left\{k_\rho I_v^{\mathrm{TM}}\right\}$
G_{yx}	$-\sin^2\psi\,\mathcal{S}_0\left\{I_i^{\mathrm{TE}}\right\} - \cos^2\psi\,\mathcal{S}_0\left\{I_i^{\mathrm{TM}}\right\} - \frac{\cos(2\psi)}{\rho}\mathcal{S}_1\left\{\frac{I_i^{\mathrm{TE}} - I_i^{\mathrm{TM}}}{k_\rho}\right\}$
G_{yy}	$\frac{\sin(2\psi)}{2}\mathcal{S}_0\left\{I_i^{\mathrm{TE}} - I_i^{\mathrm{TM}}\right\} - \frac{\sin(2\psi)}{\rho}\mathcal{S}_1\left\{\frac{I_i^{\mathrm{TE}} - I_i^{\mathrm{TM}}}{k_\rho}\right\}$
G_{yz}	$\frac{\eta_0}{\mathrm{j}k_0\varepsilon(z')}\sin\psi\,\mathcal{S}_1\left\{k_\rho I_v^{\mathrm{TM}}\right\}$
G_{zx}	$\frac{1}{\mathrm{j}k_0\eta_0\mu}\sin\psi\,\mathcal{S}_1\left\{k_\rho V_i^{\mathrm{TE}}\right\}$
G_{zy}	$-\frac{1}{\mathrm{j}k_0\eta_0\mu}\cos\psi\,\mathcal{S}_1\left\{k_\rho V_i^{\mathrm{TE}}\right\}$
G_{zz}	$\cdot$

Table 3: Scalar Green functions for computation of magnetic field due to an electric current source [2]

DGF in a similar fashion to (1):

$$\mathbf{A} = \int\limits_{r'} \underline{\underline{\mathbf{G}}}^{\mathrm{A}}(\mathbf{r}|\mathbf{r}')\mathbf{J}(\mathbf{r}')\,\mathrm{d}r', \tag{46}$$

where $\underline{\underline{\mathbf{G}}}^{\mathrm{A}}$ is the vector potential DGF. Following the formulation of [3], the spectral domain form is,

$$\underline{\underline{\tilde{\mathbf{G}}}}^{\mathrm{A}} = (\hat{\mathbf{u}}\hat{\mathbf{u}} + \hat{\mathbf{v}}\hat{\mathbf{v}})\,\tilde{G}^{\mathrm{A}}_{vv} + \hat{\mathbf{z}}\hat{\mathbf{u}}\tilde{G}^{\mathrm{A}}_{zu} + \hat{\mathbf{z}}\hat{\mathbf{z}}\tilde{G}^{\mathrm{A}}_{zz}. \tag{47}$$

The vector potential DGF is related to its fields counterpart through the magnetic field in (41) and written as:

$$\underline{\underline{\tilde{\mathbf{G}}}}^{\mathrm{HJ}} = \frac{1}{\mu}\nabla \times \underline{\underline{\tilde{\mathbf{G}}}}^{\mathrm{A}} \tag{48}$$

where isotropic permeability is assumed. To find the components of $\underline{\underline{\tilde{\mathbf{G}}}}^{\mathrm{A}}$, we first note that the 'del' operator used in the curl operation, which was initially defined in rectangular coordinates, is re-written in the spectral domain form as $\tilde{\nabla} = -\mathrm{j}k_\rho \hat{\mathbf{u}} + \hat{\mathbf{z}} d/dz$. Therefore, (48) becomes,

$$\begin{aligned}
\nabla \times \underline{\underline{\tilde{\mathbf{G}}}}^{\mathrm{A}} &= \left(-\mathrm{j}k_\rho \hat{\mathbf{u}} + \hat{\mathbf{z}} d/dz\right) \times \left[\left(\hat{\mathbf{u}}\hat{\mathbf{u}} + \hat{\mathbf{v}}\hat{\mathbf{v}}\right) \tilde{G}^{\mathrm{A}}_{vv} + \hat{\mathbf{z}}\hat{\mathbf{u}} \tilde{G}^{\mathrm{A}}_{zu} + \hat{\mathbf{z}}\hat{\mathbf{z}} \tilde{G}^{\mathrm{A}}_{zz}\right] \\
&= -\mathrm{j}k_\rho \tilde{G}^{\mathrm{A}}_{vv} \, (\hat{\mathbf{u}} \times \hat{\mathbf{v}})\hat{\mathbf{v}} + \frac{\mathrm{d}\tilde{G}^{\mathrm{A}}_{vv}}{\mathrm{d}z} \, (\hat{\mathbf{z}} \times \hat{\mathbf{u}})\hat{\mathbf{u}} - \mathrm{j}k_\rho \tilde{G}^{\mathrm{A}}_{zu} \, (\hat{\mathbf{u}} \times \hat{\mathbf{z}})\hat{\mathbf{u}} - \mathrm{j}k_\rho \tilde{G}^{\mathrm{A}}_{zz} \, (\hat{\mathbf{u}} \times \hat{\mathbf{z}})\hat{\mathbf{z}} \\
&= -\mathrm{j}k_\rho \tilde{G}^{\mathrm{A}}_{vv} \, \hat{\mathbf{z}}\hat{\mathbf{v}} + \frac{\mathrm{d}\tilde{G}^{\mathrm{A}}_{vv}}{\mathrm{d}z} \, \hat{\mathbf{v}}\hat{\mathbf{u}} + \mathrm{j}k_\rho \tilde{G}^{\mathrm{A}}_{zu} \, \hat{\mathbf{v}}\hat{\mathbf{u}} + \mathrm{j}k_\rho \tilde{G}^{\mathrm{A}}_{zz} \, \hat{\mathbf{v}}\hat{\mathbf{z}}.
\end{aligned} \tag{49}$$

Using (48) and comparing the dyads of (26b) and (49), we obtain the scalar components of the vector DGF, $\underline{\underline{\tilde{\mathbf{G}}}}^{\mathrm{A}}$:

$$\mathrm{j}\omega \tilde{G}^{\mathrm{A}}_{vv} = V^{\mathrm{TE}}_i, \tag{50a}$$

$$\mathrm{j}\omega\mu\varepsilon(z') \tilde{G}^{\mathrm{A}}_{zz} = I^{\mathrm{TM}}_v, \tag{50b}$$

$$\frac{\mathrm{d}\tilde{G}^{\mathrm{A}}_{vv}}{\mathrm{d}z} + \mathrm{j}k_\rho \tilde{G}^{\mathrm{A}}_{zu} = -\mu I^{\mathrm{TM}}_v. \tag{50c}$$

Substituting (50a) into (50c) and invoking the telegrapher's equation, (20a), we obtain:

$$\begin{aligned}
\frac{1}{\mathrm{j}\omega}\left[-\mathrm{j}k_z^{\mathrm{TE}} Z^{\mathrm{TE}} I^{\mathrm{TE}}_i\right] + \mathrm{j}k_\rho \tilde{G}^{\mathrm{A}}_{zu} &= -\mu I^{\mathrm{TM}}_v \\
\tilde{G}^{\mathrm{A}}_{zu} &= \frac{\mu}{\mathrm{j}k_\rho}\left(I^{\mathrm{TE}}_i - I^{\mathrm{TM}}_i\right),
\end{aligned} \tag{51}$$

where $Z^{\mathrm{TE}} = \omega\mu / k_z^{\mathrm{TE}}$.

1.6 Spatial domain DGFs

The spectral domain vector potentials defined in (47) can be conveniently written in a matrix form containing scalar elements,

$$\underline{\underline{\tilde{\mathbf{G}}}}^{\mathrm{A}} = \begin{bmatrix} \tilde{G}^{\mathrm{A}}_{vv} & & \\ & \tilde{G}^{\mathrm{A}}_{vv} & \\ \frac{k_x}{k_\rho}\tilde{G}^{\mathrm{A}}_{zu} & \frac{k_y}{k_\rho}\tilde{G}^{\mathrm{A}}_{zu} & \tilde{G}^{\mathrm{A}}_{zz} \end{bmatrix}. \tag{52}$$

A Fourier inversion following a similar procedure used to convert fields DGFs (35)-(39) yields the spatial domain potential DGFs expressed in terms of TLGFs, which are listed in Table. 4.

$G^{\mathrm{A}}_{xx} = G^{\mathrm{A}}_{yy}$	$\frac{1}{\mathrm{j}\omega}\mathcal{S}_0\left\{V_i^{\mathrm{TE}}\right\}$
G^{A}_{zx}	$\mathrm{j}\mu\cos\phi\,\mathcal{S}_1\left\{\frac{I_i^{\mathrm{TE}} - I_i^{\mathrm{TM}}}{k_\rho}\right\}$
G^{A}_{zy}	$\mathrm{j}\mu\sin\phi\,\mathcal{S}_1\left\{\frac{I_i^{\mathrm{TE}} - I_i^{\mathrm{TM}}}{k_\rho}\right\}$
G^{A}_{zz}	$\frac{1}{\mathrm{j}\omega\mu\varepsilon(z')}\mathcal{S}_0\left\{I_v^{\mathrm{TM}}\right\}$

Table 4: Scalar potential Green functions expressed in terms of TLGFs [9]

The above formulation is applicable to only multi-layered structure in which the layers are stacked along the x-y plane. The formulation allows insertion of arbitrarily oriented electric current source that can be placed anywhere in the structure. Once the magnetic vector potential, **A** is computed using (46), the corresponding electric and magnetic fields can be found through (45) and (41) respectively.

1.7 Computation of Transmission line Green functions

Following network analysis techniques, the voltage and current at any point in a transmission line can be obtained [4]. Each layer in the multi-layered structure is represented by a section in the transmission line which is specified by its characteristic impedance Z and the propagation constant k_z. As an example, an equivalent TL network for a semiconductor heterostructure that forms the substrate of the modern transistors is shown in Fig. 3. The layers numbered 2 and 3 in Fig. 3a are commonly made up of group III-V materials such as gallium nitride (GaN) and their subsequent alloys such aluminum gallium nitride (AlGaN). Based on the device type, the top

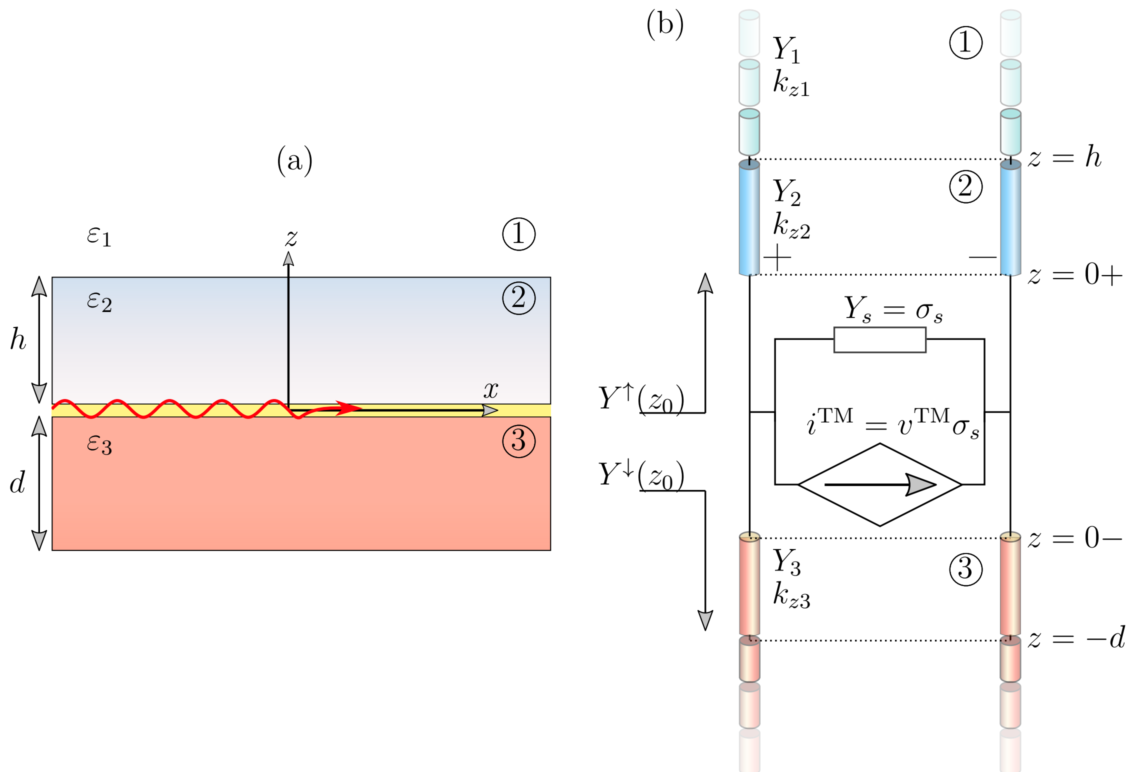

Figure 3: (a) Multilayer structure typically found in a high electron mobility transistor, (b) Equivalent transmission line network

layer labeled 1, can represent either free-space or a perfectly conducting material. The thin layer which is sandwiched between the semiconductor layers is known as a two-dimensional electron gas (2DEG) which can be visualized as a highly conductive sheet of electrons that is known to exhibit extraordinary electromagnetic properties such as highly confined surface waves [**?**, **?**]. In this section, we formulate the TLGFs for various configuration of the 2DEG and compute the respective potential Green functions.

1.7.1 Half-space

We start from the simplest case in which the 2DEG occupies the whole lower half-space. A horizontally oriented electric dipole is placed in air at a height z' from the interface where the origin is also centered. To find the component G^{A}_{xx}, we require

TE-mode voltage of an equivalent, current excited TL network which is expressed using (25a) and (25b) [4, Sec. 2.4] [3],

$$V_i^{\mathrm{TE}}(z,z') = \frac{Z_1^{\mathrm{TE}}}{2}\left[\mathrm{e}^{-\mathrm{j}k_{z1}|z-z'|} + \Gamma^{\downarrow,\mathrm{TE}}\,\mathrm{e}^{-\mathrm{j}k_{z1}(z+z')}\right], \tag{53}$$

where $\Gamma^{\downarrow,\mathrm{TE}} = (Z_{\mathrm{2DEG}}^{\mathrm{TE}} - Z_1^{\mathrm{TE}})/(Z_{\mathrm{2DEG}}^{\mathrm{TE}} + Z_1^{\mathrm{TE}})$, $Z_{\mathrm{2DEG}}^{\mathrm{TE}}$ and Z_1^{TE} are the TE mode impedances of the 2DEG and free-space regions respectively, given by (21b). The scalar potential GF, G_{xx}^{A} is then expressed as:

$$G_{xx}^{\mathrm{A}} = \mathcal{S}_0\left\{\frac{\mathrm{e}^{-\mathrm{j}k_{z1}|z-z'|}}{2\mathrm{j}k_{z1}}\right\} + \mathcal{S}_0\left\{\frac{\Gamma^{\downarrow,\mathrm{TE}}\,\mathrm{e}^{-\mathrm{j}k_{z1}(z+z')}}{2\mathrm{j}k_{z1}}\right\}. \tag{54}$$

Following similar steps, G_{zz}^{A} is found using the TM-mode current of a voltage excited network. For the components G_{zx}^{A} and G_{zy}^{A}, both the TM and TE-mode currents need to be considered for a current excited network. The final expressions are:

$$G_{zz}^{\mathrm{A}} = \mathcal{S}_0\left\{\frac{\mathrm{e}^{-\mathrm{j}k_{z1}|z-z'|}}{2\mathrm{j}k_{z1}}\right\} - \mathcal{S}_0\left\{\frac{\Gamma^{\downarrow,\mathrm{TM}}\,\mathrm{e}^{-\mathrm{j}k_{z1}(z+z')}}{2\mathrm{j}k_{z1}}\right\} \tag{55}$$

and,

$$G_{zx}^{\mathrm{A}} = \frac{\mathrm{j}\mu}{2}\cos\phi\,\mathcal{S}_1\left\{\frac{\Gamma^{\downarrow,\mathrm{TM}} - \Gamma^{\downarrow,\mathrm{TE}}}{k_\rho}\mathrm{e}^{-\mathrm{j}k_{z1}(z+z')}\right\} \tag{56}$$

References

[1] J. G. V. Bladel, *Electromagnetic Fields*, ser. IEEE Press Series on Electromagnetic Wave Theory. John Wiley & Sons, 2007.

[2] K. A. Michalski, "Electromagnetic Field Computation in Planar Multilayers," in *Encyclopedia of RF and Microwave Engineering*. John Wiley & Sons, Inc., Apr. 2005.

[3] K. Michalski and J. Mosig, "Multilayered media Green's functions in integral equation formulations," *IEEE Transactions on Antennas and Propagation*, vol. 45, no. 3, pp. 508–519, Mar. 1997.

[4] L. B. Felsen and N. Marcuvitz, *Radiation and Scattering of Waves (IEEE Press Series on Electromagnetic Wave Theory)*, ser. IEEE Press Series on Electromagnetic Wave Theory. Wiley-IEEE Press, 1994.

[5] D. G. Fang, *Antenna Theory and Microstrip Antennas*. CRC PR INC, 2010.

[6] T. Itoh, "Spectral Domain Immitance Approach for Dispersion Characteristics of Generalized Printed Transmission Lines," *IEEE Transactions on Microwave Theory and Techniques*, vol. 28, no. 7, pp. 733–736, Jul. 1980.

[7] R. Kastner, E. Heyman, and A. Sabban, "Spectral domain iterative analysis of single- and double-layered microstrip antennas using the conjugate gradient algorithm," *IEEE Transactions on Antennas and Propagation*, vol. 36, no. 9, pp. 1204–1212, 1988.

[8] M. Abramowitz and I. A. Stegun, *Handbook of Mathematical Functions*. New York: Guilford Publications, 2012.

[9] K. A. Michalski and J. R. Mosig, "The Sommerfeld half-space problem revisited: from radio frequencies and Zenneck waves to visible light and Fano modes,"

Journal of Electromagnetic Waves and Applications, vol. 5071, no. December, pp. 1–42, 2016.